CHEMISTRY
A EUROPEAN JOURNAL

DOI: 10.1002/chem.200903455

A Joint Experimental/Theoretical Investigation of the Statistical Olefin/Conjugated Diene Copolymerization Catalyzed by a Hemi-Lanthanidocene $[(Cp^*)(BH_4)LnR]$

Lionel Perrin,[a] Fanny Bonnet,*[b] Thomas Chenal,[b] Marc Visseaux,[b] and Laurent Maron*[a]

Abstract: Statistical copolymerization of ethylene and isoprene was achieved by using a borohydrido half-lanthanidocene complex. Under copolymerization conditions, activation of $[(Cp^*)(BH_4)_2Nd(thf)_2]$ ($Cp^* = \eta^5\text{-}C_5Me_5$) by an appropriate alkylating agent affords *trans*-1,4-poly-isoprene-*co*-ethylene. Analysis of the microstructure of the copolymer revealed the presence of successive short sequences of ethylene/ethylene, *trans*-1,4-isoprene/ethylene, and *trans*-1,4-isoprene/*trans*-1,4-isoprene. A small amount of 1,2-insertion of isoprene was observed, and no cyclic structures within the chain were characterized. Test runs showed that these catalysts are unable to copolymerize α-olefins (such as hex-1-ene) with isoprene. The probable initial steps in the copolymerization have been computed at the DFT level of theory. Analysis of the energy profile provides insight into the catalyst's activity and selectivity. Our theoretical results highlight the key role played by the allyl intermediate, in which diene insertion, and to a lesser extent olefin insertion, is the rate-determining step of the process. These results also illustrate the coordination behavior of the allyl ligand during the insertion of an incoming monomer, which directly inserts, after pre-coordination to the metal center, into the η^3-allyl ligand without inducing an η^3 to η^1 haptotropic shift. Finally, the inactivity of this family of catalysts towards the copolymerization of hex-1-ene was rationalized on the basis of the free-energy profile of the copolymerization.

Keywords: alkenes · copolymerization · density functional calculations · isoprene · lanthanides

Introduction

Statistical copolymerization of conjugated dienes with α-olefins is of particular interest for industrial applications,[1] because the elastomeric materials obtained exhibit improved properties compared with their parent homopolymers. However, this reaction remains a challenge to perform since these two kinds of monomers polymerize through different mechanisms. Most of the initial reports of systems that allow such copolymerizations were binary or ternary catalytic systems based on vanadium or titanium coordination complexes.[2] The first homogeneous copolymerization of butadiene and ethylene involving a metallocene was reported by Kaminsky and Schobohm, who used a zirconocene-based catalyst.[3] Since then, the copolymerization of dienes and small olefins have attracted much interest,[1,4] but published examples of the reaction have remained limited to a small number, with the majority of those utilizing rare-earth-based catalysts.[5] Among them, some examples of copolymerization of conjugated dienes with ethylene or hex-1-ene, using lanthanide-based metallocene catalysts, have been reported. Our group discovered the copolymerization of isoprene with hex-1-ene, with up to 10% hexyl units inserted within a *trans*-1,4-polyisoprene chain, by means of the ansa-samarocene complex $[(Me_2CC_5H_4)_2Sm(C_3H_5)_2Li(dme)]$.[5c]

---

[a] Dr. L. Perrin, Prof. Dr. L. Maron
LPCNO, Université de Toulouse, INSA, UPS
CNRS, LPCNO, UMR 5215 CNRS-UPS-INSA
135, avenue de Rangueil, 31077 Toulouse cedex (France)
Fax: (+33) 561-559-697
E-mail: laurent.maron@irsamc.ups-tlse.fr

[b] Dr. F. Bonnet, Dr. T. Chenal, Prof. Dr. M. Visseaux
Unité de Catalyse et de Chimie du Solide, UCCS
UMR 8181 CNRS, ENSCL, Bâtiment C7, Cité Scientifique
BP 90108, 59652 Villeneuve d'Ascq cedex (France)
Fax: (+33) 320-436-585
E-mail: fanny.bonnet@ensc-lille.fr

Supporting information for this article is available on the WWW under http://dx.doi.org/10.1002/chem.200903455.

Spitz's group then reported the ternary catalytic system $\{Me_2Si(3\text{-}SiMe_2\text{-}C_5H_3)_2\}NdCl(LiCl)(OEt_2)_2/n BuLi/(t Bu)_2AlH$, which catalyzes the copolymerization of butadiene and ethylene with up to 60 % ethylene units inserted.[5d] More recently, Carpentier et al. published the copolymerization of isoprene and ethylene with an olefin content of 24 mol %, using the single-component catalyst $[(CpCMe_2Flu)Nd(C_3H_5)(thf)]$ (Cp = cyclopentadienyl, Flu = fluorenyl).[5e] The copolymerization of butadiene with olefins was also reported in several patents from Ube Industry,[1a] Sumimoto Chemical Company,[1b] Mitsui Chemicals,[1c] and Michelin[1d] using ansa-Cp-amido and ansa-Cp-phenoxy compounds. All of these homogeneous catalytic systems exclusively involve metallocenes or constrained-geometry complexes. The half-sandwich framework based on Group 3 metals has proved highly versatile as a catalyst towards homo- and copolymerization for a wide range of apolar monomers, with very high activities and selectivities.[6] Hou et al. recently described the statistical copolymerization of isoprene and ethylene using a cationic scandium-based half-sandwich complex.[7] We report herein the first example of this kind of statistical copolymerization with a neutral half-sandwich lanthanide-based catalyst. While the homopolymerization of olefins has remained of interest, reports of copolymerization of olefin/diene systems catalyzed by lanthanidocenes and/or hemi-lanthanidocenes are rather limited. Computational approaches have provided important insights into various aspects of the mechanism of olefin homopolymerization catalyzed by Group III, IV, and lanthanide d^0 complexes.[8] However, such studies remain scarce for the cases of diene homopolymerization and monoene–diene copolymerization. In the homo- or copolymerization of butadiene, a key question is how the allyl complex, resulting from the insertion of a butadiene unit into the metal−R bond (R = growing organic chain), reacts with another olefin monomer or conjugated diene. While the η^3-coordination mode of the allyl group is the most favorable, there has been considerable discussion about a putative η^3- to η^1-haptotropic shift during the precoordination of the incoming monomer, or at its insertion transition state. This structural change may depend in a subtle way on the electronic and steric properties of the catalyst and of the reactant, which can thus be important factors in determining the preference for homo- versus copolymerization. In an early study of butadiene and isoprene copolymerization catalyzed by $[CpTiR]^+$ (used as a model for $CpTiCl_3$/MAO) (MAO = methylaluminoxane), it has been suggested, on the basis of Hartree–Fock geometry optimization, that the η^3-allyl ligand goes toward η^1-coordination during the reaction; this structural change is suggested to be rate determining.[9] Tobisch and co-workers have carried out numerous computational studies of butadiene oligomerization mostly catalyzed by electron-rich metal (Ni^{II}) complexes,[10,11] but also by $CpTi^{III}$.[12] In all cases, insertion of butadiene occurs into an η^3-allyl complex and not into an η^1-allyl complex. For the latter catalyst, further studies on the stereoselectivity of butadiene polymerization led to a similar conclusion.[12b] In the study of the tetramerization of butadiene catalyzed by Rh^I, both η^3- and η^1-allyl coordination modes have been proposed.[13] In the case of lanthanide d^0 complexes, a study of the coordination and reaction of butadiene with $[Cp^*{}_2SmH]$ has been carried out.[14] It was shown that the η^1-allyl complex is 15 kcal mol^{-1} higher in energy than the η^3-complex, and that the η^1-allyl complex corresponds to the transition state for the rotation/isomerization of the allyl ligand. It was concluded that the allyl ligand may go from η^3- to η^1-coordination during the reaction with the incoming monomer, but no computational study has yet confirmed this hypothesis. However, in a previous study on the mechanism of polystyrene polymerization catalyzed by ansa-lanthanidocenes, we demonstrated that the successive 2,1-insertions of styrene occur directly on an η^3-styrenyl ligand.[15]

Herein, we investigate the statistical copolymerization of isoprene with ethylene and hex-1-ene, using four different lanthanide half-sandwich preinitiators: $[(C_5Me_5)Sc(BH_4)_2(thf)]$ (**1**), $[(C_5Me_5)Nd(BH_4)_2(thf)_2]$ (**2**), $[(C_5Me_5)La(BH_4)_2(thf)_2]$ (**3**) and $[\{(C_5H_5)Nd(BH_4)_3\}_2][Mg(thf)_6]$ (**4**) (Scheme 1). Complexes with borohydrido groups were chosen for two reasons: 1) the BH_4 group allows the straightforward isolation of well-defined monomeric complexes;[16] and 2) in terms of catalytic efficiency, BH_4 is equivalent to a halide.[17]

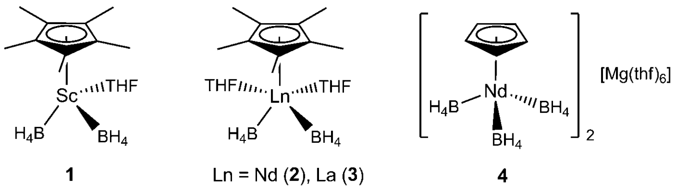

Scheme 1. Half-sandwich rare-earth based pre-initiators.

We also demonstrate that the steric hindrance induced by the presence of the aliphatic chain in hex-1-ene plays a major influence on the copolymerization. A computational study supports and rationalizes our experimental results, and allows us to propose a catalyst structure/copolymerization activity relationship. Finally, the theoretical study highlights the behavior of the allyl ligand in mono- and diene insertion reactions.

Results and Discussion

Experimental investigation of copolymerization

Statistical copolymerization attempts with isoprene and hex-1-ene by using half-sandwich lanthanide-based catalysts: Statistical copolymerization of isoprene and hex-1-ene was attempted by using borohydrido half-sandwich Group 3 and lanthanide-based complexes, such as **1**, **2**, **3**, or **4** (Scheme 1), with *n*-butylethyl magnesium (BEM) as an alkylating reagent.

Complexes **1**, **2**, and **3** were synthesized by ionic metathesis, according to published procedures,[16a–c] whereas complex **4** was prepared by using the "borohydride alkyl route," as previously reported by our group.[16d] All of these half-sandwich complexes are active and selective preinitiators towards isoprene polymerization, and lead to either highly *cis*- (with **1**[16a]) or *trans*-1,4- (with **2**,[6a] **3**[16c] or **4**[16d]) polyisoprenes. In this context, one could expect catalysts based on **2**, **3**, and **4** to insert α-olefin comonomers into the *trans*-1,4-polyisoprene structure, because catalysts able to statistically copolymerize diene and α-olefin mainly give rise to a *trans*-1,4-arrangement of diene units in the copolymer produced.[5d,18] Statistical copolymerization reactions were carried out in toluene at 50 °C over 2 to 22 h, and the results are summarized in Table 1. Except for complex **1**, which does not display any activity under these conditions, catalysts involving complexes **2**, **3**, and **4** lead to the formation of a polymeric material despite the presence of the hex-1-ene. ^{1}H and ^{13}C NMR spectroscopy revealed the formation of highly *trans*-1,4-polyisoprene, but with no hexyl units inserted within the polymer chains. The use of lithium *n*-butyl-tri-*n*-octyl aluminate instead of BEM as an alkylating reagent led to similar results (see the Supporting Information).

Table 1. Attempted statistical copolymerization of isoprene (i) with hex-1-ene (h) using **1**–**4**/BEM.[a]

Run	Cat.	[i]/[Ln]	[h]/[Ln]	Tol[b] [mL]	*t* [h]	Yield[c] [%]	h content [mol %][d]	M_n[e] [g mol^{-1}]	PDI[f]	1,4-*trans*[c] [%]
1	**1**	575	460	0.5	22	0	–	–	–	–
2	**2**	575	460	0.5	20	48	0	19100	1.36	97.5
3	**3**	575	460	0.5	20	50	0	35100	1.43	98.5
4	**4**	575	460	1	2	44	0	16500	1.66	96.5

[a] Experimental conditions: 50 °C in toluene, [Ln] = 8.7×10^{-6} mol, [Mg]/[Ln] = 1. [b] Tol refers to the volume of toluene used as a solvent. [c] Calculated taking the two monomers into account. [d] Determined by ^{1}H NMR spectroscopy in $CDCl_3$. [e] M_n corrected with factor 0.5.[19] [f] PDI = polydispersity index. Determined by gel permeation chromatography with respect to polystyrene standards.

Statistical copolymerization of isoprene with ethylene by using pre-initiator **2**: The statistical copolymerization of isoprene with ethylene was further performed by using borohydrido half-sandwich complex **2** coordinated to lithium *n*-butyl-tri-*n*-octyl aluminate (AlR_4Li; Scheme 2) as the alkylating reagent. The reaction was performed in toluene at 90 °C under an ethylene pressure of 2 bar over 1 h. Consumption of ethylene was observed, as expected, on the basis of the known ability of Ln-based catalysts to perform ethylene–diene copolymerization, as mentioned above. The copolymers obtained were analyzed by ^{1}H and ^{13}C NMR spectroscopy, which brings further insights into the microstructure of the polymer chains (see Figures 1 and 2).

The alkyl initiators (*n*-butyl or *n*-octyl) appeared in these spectra as classical alkyl groups with a greater amount of CH_2 moieties than expected. This suggests that some ethylene monomers insert into the alkyl–neodymium bonds, most probably into the initiator–neodymium bonds, during the early stages of the reaction, since ethylene activity decreases over the course of the reaction. Beside the main peaks, which can be attributed to the presence of *trans*-polyisoprene blocks, a set of neighboring peaks reveals the presence of isoprene (i) moieties close to ethylene (e) motifs (isoprene–ethylene (ie) sequences). The chemical shifts of these peaks are in accordance with published values for alternating polymers.[5e,7] Quantitatively, we observed that ethylene signals in the ie sequences have integrals four times higher than those of the alkyl initiators, while the *trans*-polyisoprene signals (ii sequences) have integrals of 20 monomer units. The aforementioned excess of CH_2 groups (ee sequences), with respect to the initiators, can be estimated at four ethylene units inserted per chain. Some defects due to 3,4-

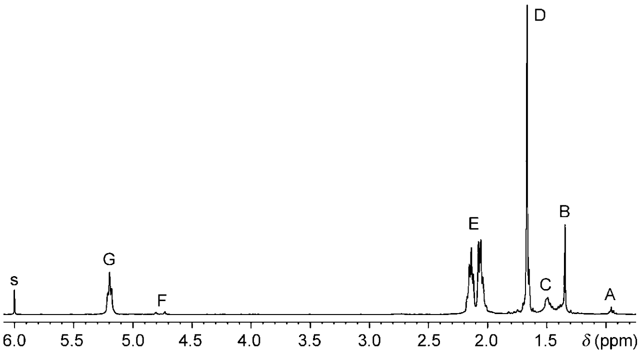

Figure 1. 1H NMR spectrum of the poly(isoprene-co-ethylene) copolymer. A) CH3 of alkyl initiators. B) CH2 of alkyl initiators and ee sequences. C) CH2 in β-position from alkenes, in ie sequences. D) CH3 of i. E) two allylic CH2 of i. F) CH2 of d (3,4-insertion of i). G) CH of i. s) solvent.

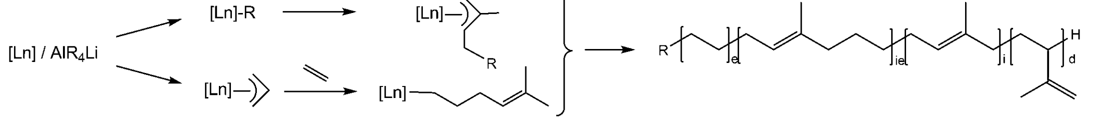

Scheme 2. Synthesis of the poly(isoprene-*co*-ethylene) copolymer. According to integration of the NMR spectra, e = 4 (ethylene inserted after initiator), ie = 4 (ethylene inserted after isoprene), i = 20 (isoprene : 1,4-*trans*-insertion) and d = 0.8 (defects : 3,4-insertion of isoprene).

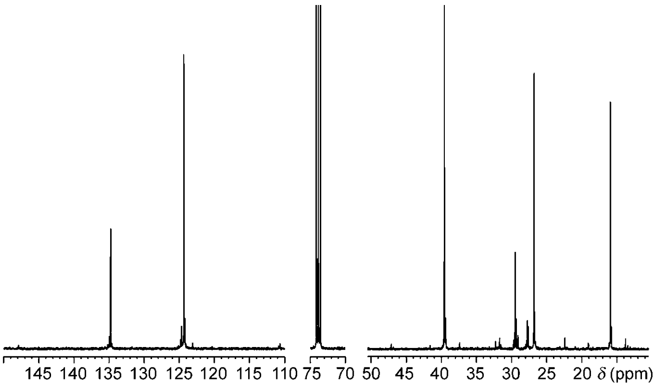

Figure 2. 13C NMR spectrum of the poly(isoprene-co-ethylene) copolymer.

insertion of isoprene (id sequences) can be detected with a mean value of 0.8 units per chain. All of these results suggest that the microstructure of the copolymer consists of chains with alkyl initiators linked, on average, to four ethylene units, followed by approximately 24 isoprene units with four ethylene units scattered within their frame (see Scheme 2).

This allows us to determine an averaged molecular weight for these oligomers of $M_n = 2000\,\text{g}\,\text{mol}^{-1}$ and an ethylene content of around 25 mol%. A reference run fed only with ethylene gave coherent results,[20] albeit the turnover frequency with pure ethylene was generally higher than for the copolymerization run. Other copolymerization runs aimed at varying the ethylene/isoprene ratio in the product resulted in the growth of either ethylene block or isoprene block polymers, but never in an increased level of ie sequences.

In summary, we have shown experimentally that ethylene behaves differently from 1-hexene in such copolymerizations: ethylene does insert, whereas 1-hexene does not. This is rationalized in the following theoretical study. It is, however, noteworthy that the presence of 1-hexene does not impede the polymerization of isoprene when both monomers are present in the reaction mixture.

Theoretical investigation of the copolymerization: The second insertion of the monomer into the active site of the catalyst has been modeled to represent the copolymerization reactions. In a first approach, ethylene and butadiene were used as simple models of α-olefin and diene, respectively. Cp and Cp* ligands have been explicitly represented and treated at the DFT level. For the purpose of clarity in the figures and simplification in the text, the $\{(\eta^5\text{-C}_5\text{Me}_5)(\eta^3\text{-BH}_4)\text{M}\}$ fragment will be denoted [M] hereafter. In all calculations, La has been selected as M, since this is realistic with respect to experiments. In addition, we have previously shown computationally that the thermodynamics and kinetics of reaction catalyzed by d^0 lanthanides are marginally affected by the nature of the lanthanide.[21] Finally, we have assumed that the catalytically active species is $[\text{Cp*}(\text{BH}_4)\text{LaR}]$ (R = alkyl or allyl) without considering additional solvent (THF) molecules coordinated to La. In a previous theoretical study, we demonstrated that decoordination of THF to the metal center is thermoneutral for this type of complex.[15]

Ethylene/butadiene copolymerization: Gibbs free energy profiles have been computed for the homopolymerization of the olefin (insertion of the olefin into an alkyl complex (Figure 3)), for the two cross insertions of copolymerization (insertion of butadiene into the alkyl complex and insertion of olefin into the allylic system (see Figure 4A and B below, respectively)) and for the homopolymerization of butadiene (*trans*-1,4- and *cis*-1,4-insertion of butadiene into the *syn*-allyl complex, (see Figure 5A and B below, respectively)). Thermodynamically, all of the reactions are computed to be favorable: $[\text{Cp*}(\text{BH}_4)\text{LaR}]$ should homo- and copolymerize both monomers, depending on the monomer feed. This is in agreement with the experiments carried out with ethylene, but not with hex-1-ene. Thus, an explicit modeling of the aliphatic chain of hex-1-ene is necessary, even in the computation of simple insertion reactions. To gain insights into the experimental results, we have analyzed the energy profiles in more detail and further investigated the effect of the hex-1-ene side chain on catalyst activity.

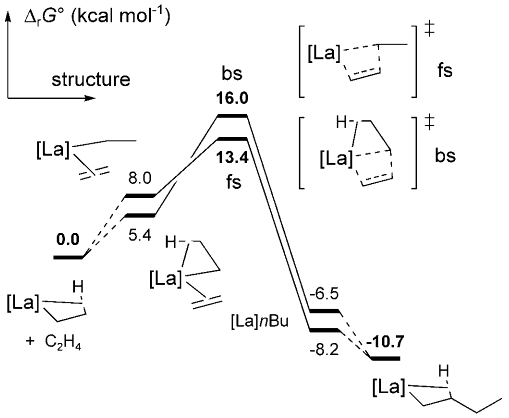

Figure 3. Gibbs free-energy profile for the homopolymerization of ethylene. [La] refers to the $\{\text{Cp*}(\text{BH}_4)\text{La}\}$ fragment, fs and bs to front-side (fs) and back-side (bs) insertion modes, respectively.

The homopolymerization of ethylene is computed to be kinetically facile with an activation barrier of 13.4 kcal mol^{-1}. For this reaction, the front-side (fs) insertion is slightly favored over the back-side insertion (bs) by 2.6 kcal mol^{-1} (Figure 3). However, the precision of the method does not allow unambiguous attribution of the regiochemistry of the insertion. This insertion is exergonic by 10.7 kcal mol^{-1}. The final product exhibits a β-C–H agostic interaction. Since a nonagostic complex was also optimized, a stabilization energy of 2.5 kcal mol^{-1} was attributed to this interaction. The low energy profile associated with this sequence of insertions is typical of a fast reaction, and it explains the successive insertions of ethylene at the early stage of the copolymerization (see the Experimental Section). This is also in agreement with the control experiment carried out with only ethylene, which revealed the high activity of the catalyst in the polymerization of ethylene. This corroboration between experiment and theory confirms the validity of our computational approach and the adequacy of the theoretical method used for studying in further detail the various initial steps involved in monoene/conjugated-diene copolymerization.

Gibbs free-energy profiles of butadiene insertions into an alkyl chain have been computed (Figure 4 A) and compared to the profile for ethylene insertion (Figure 3). For sake of clarity, only the *trans*-1,4-insertion is presented, since it is the lowest-energy pathway. The *cis*-1,4-insertion was also computed and found to be kinetically higher in energy by 1.8 kcal mol^{-1}. From the computational point of view, the *cis*-1,4-insertion mode is competitive with the *trans*-1,4-mode. This small difference in activation barrier between the two configurations has been attributed to steric effects, since the *cis*-1,4-coordination requires less steric congestion around the metal center prior to insertion to be efficient.

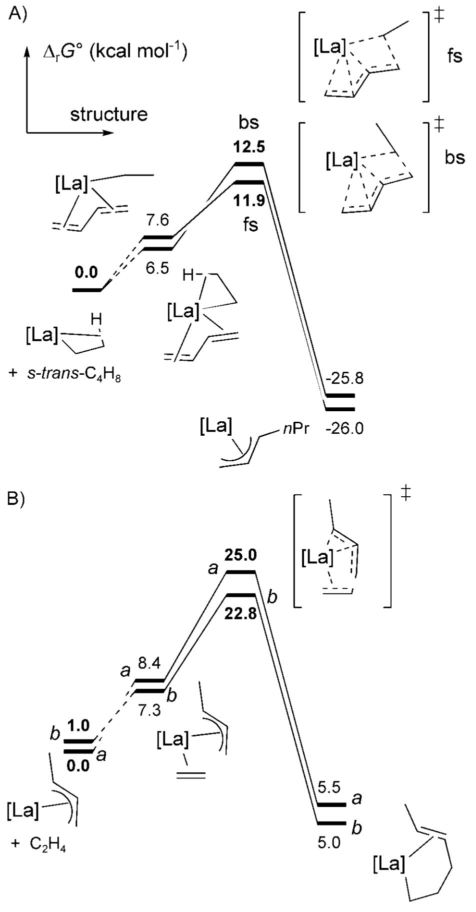

Figure 4. Free-enthalpy profiles. A) Front-side and back-side insertions of butadiene into the ethyl complex [La]Et. [La] refers to the {Cp*(BH$_4$)La} fragment. B) Insertion of ethylene into the allyl complex [La](η^3-*syn*-C$_4$H$_7$), where a and b are the facial isomers of the allyl complex [La](η^3-*syn*-C$_4$H$_7$).

As for ethylene insertion, *trans*-1,4-insertion of butadiene into the alkyl complex [La]Et is thermodynamically favorable. There is no thermodynamic discrimination between *trans*- and *cis*-1,4-insertion; both of them are exergonic by 26.0 kcal mol^{-1}, which is about 15 kcal mol^{-1} more favorable than ethylene insertion. This is due to the greater interaction between the allyl group and the metal center than between the alkyl chain and the lanthanide. The kinetics of the *trans*-1,4-butadiene insertion is characteristic of a facile reaction, with an activation barrier of 11.9 kcal mol^{-1}. According to our calculations, there is no regioselectivity in the insertion; butadiene insertions in [La]Et from the front and back sides have similar activation barriers. The activation barrier is calculated to be slightly lower (1.5 kcal mol^{-1}) for 1,4-butadiene insertion than for ethylene insertion, but this is not significant within the precision of the method. Thus, butadiene can competitively insert in a 1,4-manner into an alkyl chain to form an allyl complex with a slight preference for the *trans* isomer over the *cis*. This is in good agreement with the experimental observation that the hemilanthanidocenes tested herein yield mainly *trans*-1,4-isoprene motives in the polymer chains.

To consider all of the initial steps involved in copolymerization, it is necessary to study all possible 1,4-butadiene (Figure 5 A and B) and ethylene (Figure 4 B) insertions in

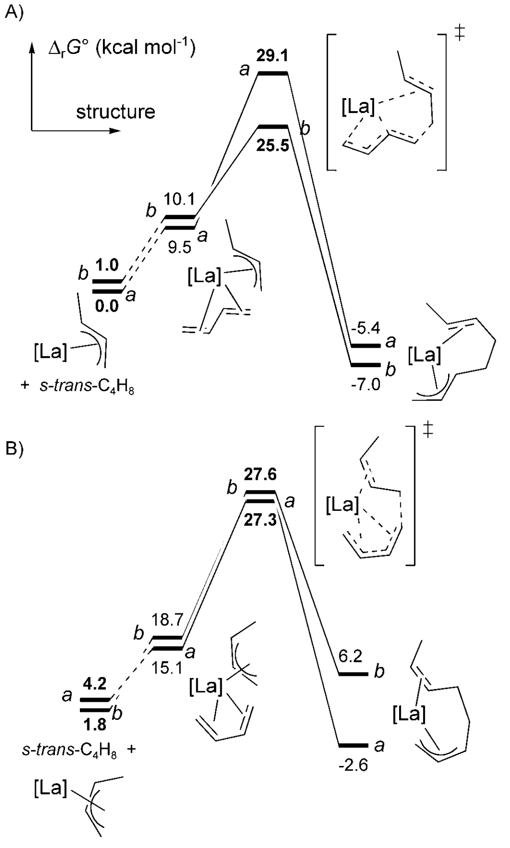

Figure 5. Gibbs free-energy profile for the *trans*-1,4- (A) and *cis*-1,4- (B) homopolymerization of butadiene. Only the supine–supine configuration has been taken into account. [La] refers to the {Cp*(BH$_4$)La} fragment.

the allyl complex [La](η^3-*syn*-C_4H_7). For butadiene insertions, from which the bb (ii experimentally) sequence arises, 1,4-*cis* and 1,4-*trans* insertions have been studied. For ethylene, insertions into the two allylic facial isomers (*a* and *b*, Figure 4B) of complex [La](η^3-C_4H_7) were considered. Since this isomerism has no effect on the energy profile, it will not be discussed in further detail.

Ethylene insertion into the allylic complex [La](*syn*-η^3-C_4H_7) is endergonic by 5.0 kcal mol^{-1}. This endergonicity partly results from the replacement of an allyl ligand by an alkyl ligand on an unsaturated metal center. However, the reaction is exothermic by about 10 kcal mol^{-1}; the difference between these two values is attributed to the loss of translational and rotational entropy of the incoming monomer during the coordination/insertion reaction. In the gas phase, these entropic effects are overestimated; thus, ethylene insertion in the allylic complex [La](*syn*-η^3-C_4H_7) should be regarded as thermoneutral. In the insertion reaction, the main-chain unsaturation yielded is coordinated to the metal center; the loss of this coordination is unfavorable by 6 kcal mol^{-1}. In the same allyl complex, the supine-*trans*-1,4-insertion of butadiene is exergonic by 7.0 kcal mol^{-1} (Figure 5A). From the kinetic point of view, both ethylene and butadiene insertions in [La](η^3-C_4H_7) are computed to be energetically accessible, although the barriers are higher than for the mono- and diene insertions into the [La]Et alkyl complex previously described. In that sense, insertion of ethylene and butadiene into the allyl complex can be viewed as the rate-determining steps of the copolymerization, and this reflects the key role played by the allyl intermediate. For the 1,4-butadiene insertion into the allyl complex, the *trans-syn* configuration is thermodynamically and kinetically slightly more favorable than the *cis-anti* one (Figure 5B). This result is in agreement with the experimental characterization of successive *trans*-1,4-polyisoprene motifs in the copolymers synthesized, although it contrasts with interpretations put forward in the literature that attribute the *cis*-polydiene sequence as a kinetic product and the *trans*-polydiene as a thermodynamic product.[22] If one considers the precision of the calculations and the difference in energy computed, such attribution cannot be discussed unambiguously.

From a mechanistic viewpoint, it should be noted that the mono- or diene insertion into the π-allyl system of [La](*syn*-η^3-C_4H_7) occurs directly and in a concerted way. There is no need to form an intermediate σ-allyl complex;[15] this was also reported by Tobisch for Ti-based catalysts.[12c]

The optimized transition-state geometry of the of the ethylene (Figure 6A) and butadiene (Figure 6B) insertions into the allyl complex [Cp*(BH_4)La(*syn*-η^3-C_4H_7)] shows that the but-2-enyl ligand is π bonded, with the La–C distance close to 2.9 Å. Similarly, the incoming monomers are η^2- and η^4-coordinated to the metal center with La–C distances ranging from 2.6 to 3.3 Å. The distance between the two carbon atoms undergoing coupling is close to 2.05 Å, which is typical of this type of transition state. It should be emphasized that no σ-bonded allyl complex could be located as a minimum on the potential energy surface. This is in agreement with previous computational studies in which the σ-allyl coordination could only be located as a transition state for isomerization between two π-allyl complexes. Thus, the insertion into the metal–allyl bond occurs on an η^3-coordinated allyl for both electron-rich and -poor metals (d^1 and d^0).[10–12]

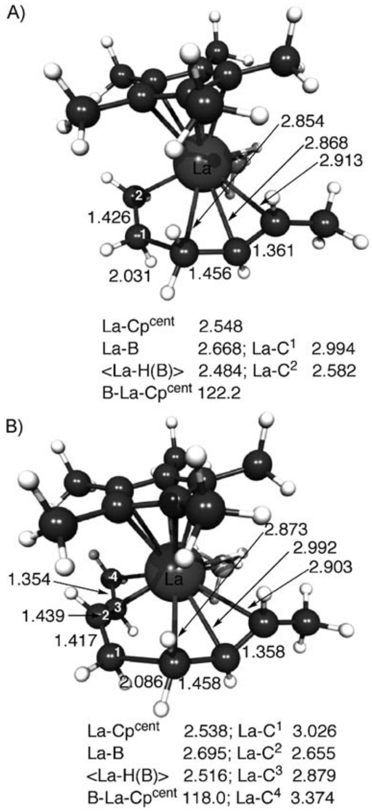

Figure 6. 3D-structure of the transition states of ethylene (A) and butadiene (B) insertions in [Cp*(BH_4)La(*syn*-η^3-C_4H_7)] and their geometrical parameters. Distances are in Å, angles in degrees. Cp^{cent} refers to the geometrical center of the Cp ring.

The free-enthalpy barrier for ethylene insertion into [La](η^3-C_4H_7) is slightly lower (by 2.7 kcal mol^{-1}) than that for the *trans*-1,4-insertion of butadiene (Figure 4B vs. 3A). Once again, this difference in energy is not significant within the precision of the method, but it does indicate a slight kinetic preference for ethylene insertion. In contrast, there is a clear thermodynamic preference for *trans*-1,4-butadiene insertion (Figure 4B vs. 3A). As a result, the butadiene–butadiene sequence is more likely to occur than the butadiene–ethylene sequence, although the latter remains possible. According to previous results,[31] if an ethylene insertion occurs, it will be followed by a 1,4-butadiene insertion, which would lead to butadiene–ethylene–butadiene sequences and an overall low ethylene content . This interpretation is in line with our experimental results, since the isoprene–isoprene sequence occurs five times more frequently in the copolymer than the isoprene–ethylene motif, with an ethylene content of about 25 mol %.

At this stage, our theoretical approach is consistent with, and helps to rationalize, our experimental observations. More sophisticated approaches, involving kinetic models, could be utilized for this purpose. However, inserting our barriers into a kinetic model for copolymerization (Scheme 3)[23] leads to similar conclusions ($r_1r_2=0.8\times10^{-3}$ with $r_1=79.5\times10^{-3}$ and $r_2=10.5\times10^{-3}$).

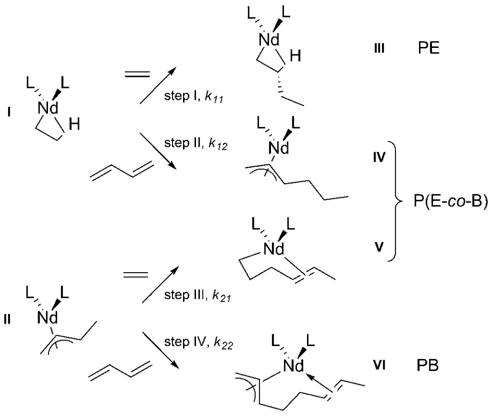

Scheme 3. Modeled propagation steps involved in ethylene homopolymerization (step I), ethylene–butadiene copolymerization (steps II and III) and butadiene homopolymerization (step IV); k_{ij} are the rate constants of the insertion reactions. PE: polyethylene, PB: polybutadiene, P(E-*co*-B): ethylene-*co*-butadiene (statistical copolymer).

The form of the catalyst is an important issue. Thus far, we have only considered that the magnesium complex is exchanging one ligand with the lanthanide complex. However, the remaining BH_4 ligand on the lanthanide fragment could also be displaced by the Mg complex to form either a bis-alkyl or an allyl–alkyl complex. Therefore, we carried out a similar computational study with these two putative complexes to check the likelihood of their formation. The activation barriers for the four considered processes were computed (see Table 2).

Table 2. Computed activation barriers for the three possible complexes in kcal mol^{-1}.

Reaction	Cp(BH_4)	Cp(Et)	Cp(C_3H_5)
ethylene insertion into Ln–Et	13.4	14.1	17.2
butadiene insertion into Ln–Allyl	25.5	24.3	27.3
butadiene insertion into Ln–Et	11.9	13.6	17.2
ethylene insertion into Ln–Allyl	22.8	25.5	22.1

The three complexes are predicted to react in an analogous way with similar activation barriers, and the results do not change our conclusion on the possible copolymerization.

In summary, the copolymerization is mainly under thermodynamic control, because all possible reactions are kinetically accessible. The formation of the highly stable π-allyl complex, rather than the alkyl complex, controls the kinetics of the reaction and induces the microstructure of the resulting copolymer. Additionally, the reaction is guided by a subtle balance between steric factors around the metal center, which explains the slight preference for the *trans*-1,4-insertion over *cis*-1,4-insertion of butadiene. The acidic character of the metal center also accounts for efficiency of the catalyst in the mono-/diene copolymerization. Indeed, metallocene complexes that do not contain an ansa arm, where the steric hindrance is higher and the charge of the metal fragment is lower,[24] have never been reported, to the best of our knowledge, to allow efficient statistical copolymerization of olefins and conjugated dienes.

Hex-1-ene/butadiene copolymerization: Discrepancies between experimental results for the isoprene/hex-1-ene copolymerization and theoretical calculations based on ethylene and butadiene revealed the inadequacy of the structural modeling along a side-chain α-olefin by ethylene. To address this point, we investigated the influence of the *n*-butyl chain on the reactivity of the catalyst. The free-enthalpy profiles of hex-1-ene homopolymerization (Figure 7) and hex-1-ene/butadiene copolymerization (Figure 8) have been computed.

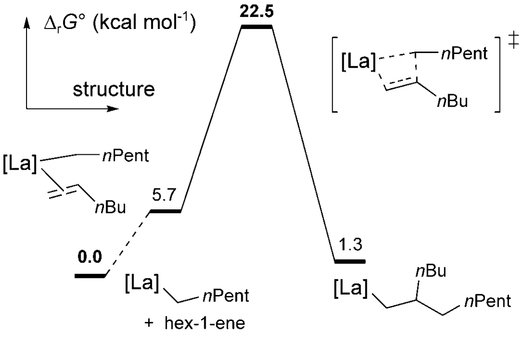

Figure 7. Gibbs free-energy profile for the homopolymerization of hex-1-ene by 1,2-front-side insertion. [La] refers to the {Cp*(BH_4)La} fragment.

Among the four steps implied in mono-/diene copolymerization, the major difference between the free-enthalpy profiles computed for hex-1-ene and ethylene is caused by the difference in thermodynamics for the olefin insertion into the π-allylic intermediate complex (Figure 8B). This initial step is endergonic by 13.5 kcal mol^{-1} and hence cannot occur. As a consequence, no insertion of hex-1-ene is expected in the *trans*-1,4-polybutadiene. This is in agreement with our experimental observations. Kinetically, the front-side 1,2-insertion of hex-1-ene into the hexyl complex [Cp*(BH_4)La(*n*-Hex)] is less facile than the equivalent ethylene insertion. An activation barrier of 22.5 kcal mol^{-1} has been computed for hex-1-ene insertion in [La]Et, which is 9 kcal mol^{-1} higher than that computed for ethylene insertion in [La]Et. This reaction is also computed to be marginally endergonic by 1.3 kcal mol^{-1}, whereas it is clearly exergonic in the case of ethylene (−10.7 kcal mol^{-1}). This trend is in agreement with the previous work of Barros et al.[25] on the hydromethylation of propene by [Cp_2MCH_3] (M = Sc or Lu), where calculations revealed that the second insertion of an α-olefin was not competitive with hydromethylation for kinetic reasons. On the other hand, *trans*-1,4-insertion of bu-

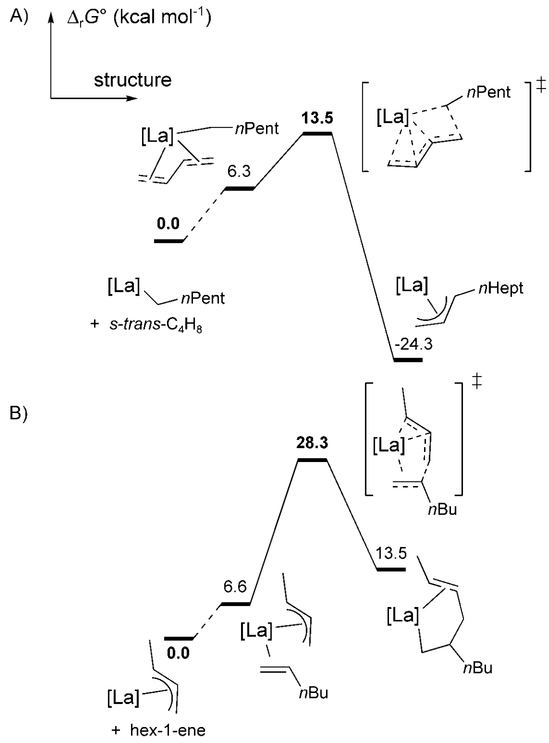

Figure 8. Gibbs free-energy profiles for the initial steps of the cross insertion of butadiene/*n*-hex-1-ene copolymerization. A) 1,4-*trans* insertion of butadiene into [La]Et; B) hex-1-ene insertion into [La](η^3-C_4H_7). [La] refers to the {Cp*(BH_4)La} fragment.

tadiene into the hexyl complex [Cp*(BH_4)La(*n*-Hex)] is computed to be as facile as its equivalent insertion into the ethyl complex [Cp*(BH_4)La(Et)]. This indicates that the ethyl group is a reasonable model for the hexyl radical.

Conclusion

In this study, a joint experimental/theoretical investigation of the olefin–diene copolymerization activity of [Cp*(BH_4)LnR] complexes is reported. It was possible to achieve ethylene–isoprene copolymerization, which led to partially statistical copolymers of *trans*-1,4-polyisoprene-*co*-ethylene. This is, to the best of our knowledge, the first report of such activity with a hemimetallocene complex. On the other hand, no hex-1-ene insertion was observed in the polymeric product, and pure *trans*-1,4-polyisoprene was obtained. Our computational study was able to reproduce and explain these findings. Indeed, it was found that *trans*-1,4-butadiene insertion into an alkyl complex is the most favored reaction, both thermodynamically and kinetically. This reaction leads to the formation of a highly stable allyl complex. According to our calculations, insertion of ethylene into the allylic system is marginally disfavored thermodynamically, but kinetically favored with respect to the 1,4-insertion of butadiene into the allyl complex, which is thermodynamically more favorable. This explains the formation of the statistical copolymer. A subtle balance between steric and electronic effects controls this reaction. Even better reactivity is expected with a less bulky Cp ligand. The preference for the *trans*-1,4-insertion is reproduced theoretically, and is associated with the steric hindrance around the metal center.

The case of hex-1-ene was also rationalized. Hex-1-ene insertion into an allyl complex is calculated to be endergonic by 14 kcal mol^{-1}, which prevents hex-1-ene insertion. Experimentally, *trans*-1,4-poly-isoprene is obtained under copolymerization conditions. Finally, ethylene cannot be considered to be a realistic model for α-olefin, even for simple insertion reactions.

Experimental Section

Computational details: Lanthanum was represented with a Stuttgart–Dresden pseudopotential that includes the 4f electrons in the core in combination with its adapted basis set.[26] This basis set was augmented by a set of f polarization functions ($\alpha = 1.000$). All carbon, boron, and hydrogen atoms have been described with an all-electron 6-311G(d,p) triple-ζ basis set,[27a,b] except the carbon and hydrogen atoms of Cp* methyl groups, which were represented with an all-electron 6-31G triple-ζ basis set.[27c] Calculations were carried out at the DFT level of theory using the hybrid functional B3PW91.[28] Geometry optimizations were carried out without any symmetry restrictions, and the nature of the minima was verified with analytical frequency calculations. For all transition states, the intrinsic reaction coordinate was followed according to the intrinsic reaction coordinate technique, and the thermodynamic data were obtained within the harmonic approximation at $T = 298.15$ K. All these computations have been performed with the Gaussian 03[29] suite of programs.

Materials: All operations were performed under dry argon with Schlenk techniques. Solvents were dried over sodium/benzophenone ketyl, deoxygenated, and stored over molecular sieves (3 Å) in a glove box. Hex-1-ene and isoprene (99% from Aldrich) were dried over calcium hydride, distilled twice, and stored over molecular sieves (3 Å) in a glove box. BEM (20% solution in hexanes) from Texas Alkyl was used as received. Ethylene (from Air Liquide, 99.95% purity, O_2 and H_2 <10 ppm, H_2O and CO_2 <5 ppm) was used as received. Lithium *n*-butyl-tri-*n*-octyl aluminate was synthesized by following a literature procedure[30] using tri-*n*-octyl aluminum (from Schering) and *n*-butyl lithium in 1.6 M hexane solution (from Aldrich). Complexes **1**–**4** were all synthesized according to literature procedures.[16] ^{1}H and ^{13}C NMR spectra of the polyisoprenes were recorded on a Bruker Advance 300 spectrometer in $CDCl_3$ and on a Bruker AC 400 spectrometer in $C_2D_2Cl_4$ solutions at 130 °C for the isoprene–ethylene copolymer.

Typical isoprene/hex-1-ene statistical copolymerization: In a glove box under argon (H_2O and O_2 <2 ppm), the half-sandwich pre-initiator was dissolved in toluene (dry and degassed; 0.5 or 1 mL). Isoprene (0.5 mL) mixed with hex-1-ene (0.5 mL) was then added, followed by BEM (1 equiv). The reaction was then stirred and heated at 50 °C for a given time. The reaction was quenched by the dropwise addition of methanol. The polymer was then poured into a large excess of methanol, filtered, and dried under vacuum. ^{1}H and ^{13}C NMR spectroscopy of the polymers in $CDCl_3$ revealed that no hex-1-ene was inserted into the polymer chain, and that only pure polyisoprene was obtained, except in run 1 in which no polymer was formed.

Isoprene–ethylene statistical copolymerization: In a glove box, the neodymium preinitiator **2** (22.7 mg, 50 μmol) was dissolved in toluene (4 mL), and drawn up into a syringe. Lithium *n*-butyl-tri-*n*-octyl aluminate (107.7 mg, 250 μmol) was dissolved in isoprene (2.4 g), drawn up into a syringe, and made up to 16 mL with toluene. The aluminate solution was injected into the polymerization reactor at 90 °C under an atmospheric pressure of ethylene, before the absolute pressure was raised to 2.0 bar. An ethylene inlet allowed continuous saturation of the inner medium at constant pressure. The neodymium solution was then injected to start the polymerization, and the ethylene consumption was monitored with a flowmeter. Initial activity was near $10\,kg\,C_2H_4\,h^{-1}\,mol^{-1}\,Nd$, and was followed by an exponential decrease. After 1 h, the green homogeneous mixture was poured into methanol (100 mL with 15 mg of butylated hydroxytoluene, as antioxidizer). The polymer was then separated from the solution, dried, and weighed (1.10 g). Integration of the flowmeter signal gave the mass of consumed ethylene (0.16 g), which allowed the calculation of the mean turnover frequency (TOF) for ethylene insertion: $TOF_{ethylene} = 110\,h^{-1}$. After deducting the mass of consumed ethylene and of the initiating alkyl species, the resulting mass of polymer consists of reacted isoprene. Thus, the conversion rate and the mean TOF for isoprene can be calculated: $r = 35\,\%$, $TOF_{isoprene} = 250\,h^{-1}$.

Acknowledgements

We are grateful to the CNRS, UPS, and CEA for financial support of this work. CalMip (CNRS, Toulouse, France) is acknowledged for use of calculation facilities. L.M. thanks the Institut Universitaire de France. The authors would like to thank A. Malfait for the gel permeation chromatographic analyses of the polymers and P. Zinck for the synthesis of complex **3**.

---

[1] a) Ube Industries, Ltd. , JP 10237131, **1998**; [S. Ikai, E. Narisawa, *Chem. Abstr.* **1998**, *129*, 231171e]; b) Sumitoro Chemical Co. , US 6288191, **2001**; [T. Nishiyama, A. Ogawa, *Chem. Abstr.* **1999**, *131*, 244494d]; c) Mitsui Chemicals, EP 891993, **1999**; [K. Morizono, K. Okada, M. Yamaguchi, *Chem. Abstr.* **1999**, *130*, 111426r]; d) Michelin Recherche, Atofina Research, WO 035639, **2004**; [V. Monteil, R. Spitz, C. Boisson, *Chem. Abstr.* **2004**, *140*, 340585].

[2] a) G. Natta, A. Zambelli, I. Pasquon, F. Ciampelli, *Makromol. Chem.* **1964**, *79*, 161–169; b) J. Furukawa, E. Kobayashi, *Rubber Chem. Technol.* **1978**, *51*, 600–646; c) W. Kuran, *Principles of Coordination Polymerization*, 1st ed., Wiley, New York, **2001**.

[3] W. Kaminsky, M. Schobohm, *Macromol. Symp.* **1986**, *4*, 103–118.

[4] For example, see: a) W. Kaminsky, B. Hinrichs, *Macromol. Symp.* **2003**, *195*, 39–44; b) S. Pragliola, C. Costabile, M. Napoli, G. Guerra, P. Longo, *Macromol. Symp.* **2006**, *234*, 128–138; c) C. Capacchione, A. Avagliano, A. Proto, *Macromolecules* **2008**, *41*, 4573–4575.

[5] a) R. K. Kudashev, E. A. Glukhov, R. R. Muslukhov, Y. B. Monakov, R. Rafikov, *Dokl. Phys. Chem.* **1989**, *308*, 1398–1401; b) R. Kaulbach, U. Gebauer, K. Gehrke, M. D. Lachner, K. Hummel, *Angew. Makromol. Chem.* **1995**, *226*, 101–109; c) D. Barbier-Baudry, A. Dormond, P. Desmurs, *C. R. Acad.*, *Serie IIc* **1999**, 2, 375–378; d) F. Barbotin, V. Monteil, M. F. Llauro, C. Boisson, R. Spitz, *Macromolecules* **2000**, *33*, 8521–8523; e) A. S. Rodrigues, E. Kirillov, B. Vuillemin, A. Razavi, J. F. Carpentier, *Polymer* **2008**, *49*, 2039–2045.

[6] For selected references, see: a) F. Bonnet, M. Visseaux, A. Pereira, D. Barbier-Baudry, *Macromolecules* **2005**, *38*, 3162–3169; b) Z. Hou, Y. Luo, X. Li, *J. Organomet. Chem.* **2006**, *691*, 3114–3121; c) J. Hitzbleck, K. Beckerle, J. Okuda, T. Halbach, R. Mülhaupt, *Macromol. Symp.* **2006**, *236*, 23–29; d) M. Zimmermann, K. W. Törnroos, R. Anwander, *Angew. Chem.* **2008**, *120*, 787–790; *Angew. Chem. Int. Ed.* **2008**, *47*, 775–778; e) N. Yu, M. Nishiura, X. Li, Z. Xi, Z. Hou, *Chem. Asian J.* **2008**, *3*, 1406–1414.

[7] X. Li, M. Nishiura, L. Hu, K. Mori, Z. Hou, *J. Am. Chem. Soc.* **2009**, *131*, 13870–13882.

[8] a) P. Margl, L. Deng, T. Ziegler, *Organometallics* **1998**, *17*, 933–946; b) P. Margl, L. Deng, T. Ziegler, *J. Am. Chem. Soc.* **1998**, *120*, 5517–5525; c) H. Kawamura-Kuribayashi, N. Koga, K. Morokuma, *J. Am. Chem. Soc.* **1992**, *114*, 2359–2366; d) H. Kawamura-Kuribayashi, N. Koga, K. Morokuma, *J. Am. Chem. Soc.* **1992**, *114*, 8687–8694; e) L. Petitjean, D. Pattou, M. F. Ruiz-López, *J. Mol. Struct.* **2001**, *541*, 227–235; f) L. Petitjean, D. Pattou, M. F. Ruiz-López, *Tetrahedron* **2001**, *57*, 2769–2774; g) P. Margl, L. Deng, T. Ziegler, *J. Am. Chem. Soc.* **1999**, *121*, 154–162; h) L. Cavallo, G. Guerra, *Macromolecules* **1996**, *29*, 2729–2737; i) P. Margl, J. C. W. Lohrenz, T. Ziegler, P. E. Blochl, *J. Am. Chem. Soc.* **1996**, *118*, 4434–4441; j) E. Zurek, T. Ziegler, *Organometallics* **2002**, *21*, 83–92, and references therein; k) K. Vanka, T. Ziegler, *Organometallics* **2001**, *20*, 905–913; l) M. Borrelli, V. Busico, R. Cipullo, S. Ronca, P. H. M. Budzelaar, *Macromolecules* **2002**, *35*, 2835–2844; m) T. K. Woo, L. Fan, T. Ziegler, *Organometallics* **1994**, *13*, 432–433; n) T. Yoshida, N. Koga, K. Morokuma, *Organometallics* **1995**, *14*, 746–758.

[9] a) A. Peluso, R. Improta, A. Zambelli, *Organometallics* **2000**, *19*, 411–419; b) A. Peluso, R. Improta, A. Zambelli, *Macromolecules* **1997**, *30*, 2219–2227.

[10] a) S. Tobisch, *J. Am. Chem. Soc.* **2004**, *126*, 259–272; b) S. Tobisch, *Adv. Organomet. Chem.* **2003**, *49*, 167–224; c) S. Tobisch, *Chem. Eur. J.* **2003**, *9*, 1217–1232; d) S. Tobisch, T. Ziegler, *J. Am. Chem. Soc.* **2002**, *124*, 13290–13301; e) S. Tobisch, T. Ziegler, *J. Am. Chem. Soc.* **2002**, *124*, 4881–4893.

[11] a) S. Tobisch, R. Taube, *J. Organomet. Chem.* **2003**, *683*, 181–190; b) S. Tobisch, *Macromolecules* **2003**, *36*, 6235–6244; c) S. Tobisch, *Chem. Eur. J.* **2002**, *8*, 4756–4766; d) S. Tobisch, *Acc. Chem. Res.* **2002**, *35*, 96–104; e) S. Tobisch, R. Taube, *Chem. Eur. J.* **2001**, *7*, 3681–3695; f) S. Tobisch, R. Taube, *Organometallics* **1999**, *18*, 5204–5218; g) S. Tobisch, R. Taube, *Organometallics* **1999**, *18*, 3045–3060; h) S. Tobisch, H. Bogel, R. Taube, *Organometallics* **1998**, *17*, 1177–1196; i) H. Bogel, S. Tobisch, *Int. J. Quantum Chem.* **1996**, *60*, 197–205; j) S. Tobisch, H. Bogel, R. Taube, *Organometallics* **1996**, *15*, 3563–3571.

[12] a) S. Tobisch, *Organometallics* **2003**, *22*, 2729–2740; b) C. Costabile, G. Milano, L. Cavallo, G. Guerra, *Macromolecules* **2001**, *34*, 7952–7960; c) S. Tobisch, *J. Mol. Struct.* **2006**, *771*, 171–179.

[13] S. Tobisch, H. Werner, *Dalton Trans.* **2004**, 2963–2968.

[14] S. Kaita, N. Koga, Z. Hou, Y. Doi, Y. Wakatsuki, *Organometallics* **2003**, *22*, 3077–3082.

[15] L. Perrin, Y. Sarazin, E. Kirilov, J. F. Carpentier, L. Maron, *Chem. Eur. J.* **2009**, *15*, 3773–3783.

[16] a) F. Bonnet, C. Da Costa Violante, P. Roussel, A. Mortreux, M. Visseaux, *Chem. Commun.* **2009**, 3380–3382; b) S. Cendrowski-Guillaume, G. Le Gland, M. Nierlich, M. Ephritikine, *Organometallics* **2000**, *19*, 5654–5660; c) P. Zinck, A. Valente, A. Mortreux, M. Visseaux, *Macromol. Rapid Commun.* **2009**, *30*, 528–531; d) M. Visseaux, P. Zinck, M. Terrier, A. Mortreux, P. Roussel, *J. Alloys Compd.* **2008**, *451*, 352–357.

[17] a) M. Visseaux, T. Chenal, P. Roussel, A. Mortreux, *J. Organomet. Chem.* **2006**, *691*, 86–92; b) J. Thuilliez, R. Spitz, C. Boisson, *Macromol. Chem. Phys.* **2006**, *207*, 1727–1731.

[18] M. Visseaux, D. Barbier-Baudry, F. Bonnet, A. Dormond, *Macromol. Chem. Phys.* **2001**, *202*, 2485–2488.

[19] P. Zinck, M. Terrier, A. Mortreux, M. Visseaux, *Polym. Test.* **2009**, *28*, 106–108.

[20] 1.42 g of pure polyethylene was recovered, initial activity = $275\,kg\,PE\,mol^{-1}\,Nd\,h^{-1}$.

[21] a) L. Maron, L. Perrin, O. Eisenstein, *Dalton Trans.* **2003**, 4313–4318; b) L. Perrin, L. Maron, O. Eisenstein, *Inorg. Chem.* **2002**, *41*, 4355–4362; c) L. Maron, L. Perrin, O. Eisenstein, *J. Chem. Soc. Dalton Trans.* **2002**, 534–539.

[22] D. J. Wilson, *Polym. Int.* **1996**, *39*, 235–242.

[23] G. Odian, *Principles of Polymerization*, 3rd ed., Wiley, New York, **1991**, p. 452.

[24] L. Perrin, L. Maron, O. Eisenstein, *New J. Chem.* **2004**, *28*, 1255–1259.

[25] N. Barros, O. Eisenstein, L. Maron, T. D. Tilley, *Organometallics* **2006**, *25*, 5699–5708.

[26] a) M. Dolg, H. Stoll, A. Savin, H. Preuss, *Theor. Chim. Acta* **1989**, *75*, 173–194; b) M. Dolg, H. Stoll, H. Preuss, *Theor. Chim. Acta* **1993**, *85*, 441–450.

[27] a) A. D. McLeann, G. S. Chandler, *J. Chem. Phys.* **1980**, *72*, 5639–5648; b) K. Raghavachari, J. S. Binkley, R. Seeger, J. A. Pople, *J. Chem. Phys.* **1980**, *72*, 650–654; c) R. D. Ditchfield, W. J. Hehre, J. A. Pople, *J. Chem. Phys.* **1971**, *54*, 724–728.

[28] a) J. P. Perdew, Y. Wang, *Phys. Rev. B* **1992**, *82*, 284–298; b) A. D. Becke, *J. Chem. Phys.* **1993**, *98*, 5648–5652.
[29] Gaussian 03, Revision C.02, M. J. Frisch, G. W. Trucks, H. B. Schlegel, G. E. Scuseria, M. A. Robb, J. R. Cheeseman, J. A. Montgomery, Jr., T. Vreven, K. N. Kudin, J. C. Burant, J. M. Millam, S. S. Iyengar, J. Tomasi, V. Barone, B. Mennucci, M. Cossi, G. Scalmani, N. Rega, G. A. Petersson, H. Nakatsuji, M. Hada, M. Ehara, K. Toyota, R. Fukuda, J. Hasegawa, M. Ishida, T. Nakajima, Y. Honda, O. Kitao, H. Nakai, M. Klene, X. Li, J. E. Knox, H. P. Hratchian, J. B. Cross, V. Bakken, C. Adamo, J. Jaramillo, R. Gomperts, R. E. Stratmann, O. Yazyev, A. J. Austin, R. Cammi, C. Pomelli, J. W. Ochterski, P. Y. Ayala, K. Morokuma, G. A. Voth, P. Salvador, J. J. Dannenberg, V. G. Zakrzewski, S. Dapprich, A. D. Daniels, M. C. Strain, O. Farkas, D. K. Malick, A. D. Rabuck, K. Raghavachari, J. B. Foresman, J. V. Ortiz, Q. Cui, A. G. Baboul, S. Clifford, J. Cioslowski, B. B. Stefanov, G. Liu, A. Liashenko, P. Piskorz, I. Komaromi, R. L. Martin, D. J. Fox, T. Keith, M. A. Al-Laham, C. Y. Peng, A. Nanayakkara, M. Challacombe, P. M. W. Gill, B. Johnson, W. Chen, M. W. Wong, C. Gonzalez, J. A. Pople, Gaussian, Inc., Wallingford CT, **2004**.
[30] E. C. Ashby, G. E. Heinsohn, *J. Org. Chem.* **1973**, *38*, 4343–4344.
[31] L. Perrin, L. Maron, Abstract ACS Meeting, **2010**.

Received: December 17, 2009
Revised: June 8, 2010